Available at
www.ElsevierComputerScience.com
POWERED BY SCIENCE DIRECT®

Neural Networks 17 (2004) 225–232

Neural Networks

www.elsevier.com/locate/neunet

Bifurcating neuron: computation and learning

Mykola Lysetskiy, Jacek M. Zurada*

Department of Electrical and Computer Engineering, University of Louisville, Louisville, KY 40292, USA

Received 18 June 2002; revised 24 September 2003; accepted 24 September 2003

Abstract

The ability of bifurcating processing units and their networks to rapidly switch between different dynamic modes has been used in recent research efforts to model new computational properties of neural systems. In this spirit, we devise a bifurcating neuron based on control of chaos collapsing to a period-3 orbit in the dynamics of a quadratic logistic map (QLM). Proposed QLM3 neuron is constructed with the third iterate of QLM and uses an external input, which governs its dynamics. The input shifts the neuron's dynamics from chaos to one of the stable fixed points. This way the inputs from certain ranges (clusters) are mapped to stable fixed points, while the rest of the inputs is mapped to chaotic or periodic output dynamics. It has been shown that QLM3 neuron is able to learn a specific mapping by adaptively adjusting its bifurcation parameter, the idea of which is based on the principles of parametric control of logistic maps [Proceedings of the International Symposium on Nonlinear Theory and its Applications (NOLTA'97), Honolulu, HI, 1997; Proceedings of SPIE, 2000]. Learning algorithm for the bifurcation parameter is proposed, which employs the error gradient descent method.
© 2003 Elsevier Ltd. All rights reserved.

Keywords: Bifurcating neuron; Quadratic logistic map; Chaotic attractor; Saddle-node bifurcation; Period-3 orbit window

1. Introduction

Limitations of the static nature of artificial neural networks (ANN) stimulate investigation of biologically motivated neuron models with inherent dynamics, such as bifurcating and chaotic neurons (Farhat, 2000; Farhat & Eldefrawy, 1992; Farhat, Lin, & Eldefrawy, 1994; Holden, Hyde, Muhamad, & Zhang, 1992). In the networks composed of such neurons information is processed by convergence not only to a fixed point, but also to a limit cycle or chaotic attractor (Farhat, 2000; Farhat, Lee, & Ling, 1998; Hirsch & Baird, 1995; Lee & Farhat, 2001).

Artificial neurons commonly used to mimic dynamics of biological neurons are simplified versions of the Hodgkin-Huxley type model (HHM), such as, for instance, integrate-and-fire neurons. These models demonstrate very rich dynamics, with a variety of bifurcations and chaotic phenomena (Farhat & Eldefrawy, 1992; Farhat et al., 1994; Feudel et al., 2000; Holden et al., 1992; Izhikevich, 2000). For example, dynamics of interspike time interval of biological thermally sensitive neurons with increasing temperature (which is both its input and bifurcation parameter), undergoes transition to chaos via period-doubling cascade, intermittency and crises of chaotic attractors, emerging windows of periodic activity, etc. as shown in Fig. 1. (Feudel et al., 2000).

More typically, chaotic neural dynamics emerges at macro-level, in the network of dynamical units. Seminal results of Freeman and co-workers (Freeman, 1988) suggest that the state of the olfactory bulb in olfactory system, when unperturbed, is wandering within high-dimensional chaotic attractor. Applied input (odor) shifts the system to one of its low-dimensional attractors, 'wings', that correspond to the recognized odor.

Dynamics of the network of parametrically coupled logistic maps was explored in (Farhat, 1997, 2000; Farhat et al., 1998). It was shown that such networks may have enormous memory capacity due to the astronomical number of different coexisting dynamic attractors. The lattices of chaotic maps were studied in Dmitriev, Shirokov, and Starkov (1997), Kaneko and Tsuda (2000) and Sinha and Ditto (1998). Chaotic dynamics of a network was also explored in Adachi and Aihara (1997) and Hoshino, Usaba, Kashimori, and Kambara (1997), and applied to an engineering application: a search of an optimal solution of the traveling salesman problem (Tokuda, Nagashima, & Aihara, 1997). Encoding with the trajectory of the system's

* Corresponding author.
E-mail address: j.mzura02@louisville.edu, (J.M. Zurada).

0893-6080/$ - see front matter © 2003 Elsevier Ltd. All rights reserved.
doi:10.1016/j.neunet.2003.09.003

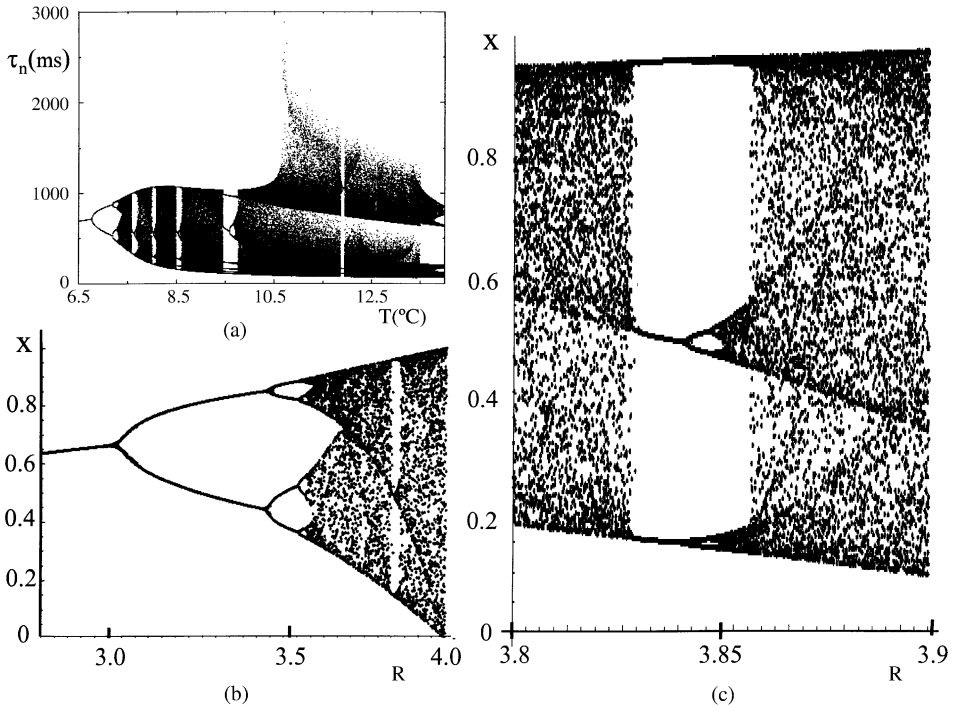

Fig. 1. (a) Bifurcation diagram of the modified Hodgkin-Huxley model of the thermally sensitive neuron. Interspike intervals τ_n versus bifurcation parameter, temperature T (From Feudel et al., (2000). *Chaos*, 10(1)). (b) Bifurcation diagram of quadratic logistic map $x_{t+1} = Rx_t(1 - x_t)$, x_t values versus bifurcation parameter R. (c) Zoomed in version of (b): Emerging of period-3 orbit.

state in the phase space realized in a network of FitzHugh–Nagumo spiking neurons was studied in Rabinovich et al. (2001).

In biological neural circuits, input may not be presented by initial conditions. It is, rather, one of the bifurcation parameters (Feudel et al., 2000; Fukai, Doi, Nomura, & Sato, 2000; Koch, 1999). Dynamics of thermally sensitive neurons (Braun, Eckhardt, Braun, & Huber, 2000; Feudel et al., 2000; Gilmore et al., 1999) is a good illustration of this idea. This input-as-a-bifurcation-parameter concept, explored in Farhat and Eldefrawy (1992), Farhat et al. (1994) and Holden et al. (1992) provides an insight of how microscopic fluctuations of an input may be able to change the system's global dynamics.

1.1. Why maps?

Biologically realistic modified Hodgkin-Huxley neuron models are barely analytically tractable due to a huge number of variables and bifurcation points. However, certain aspects of their activity, for example, the dynamics of the interspike time intervals, can often be described with dynamics of sine-circle and other maps, which are, generally, easier to work with Ermentrout and Kopell (1998) and Farhat and Eldefrawy (1992, 1994). In this article, as in Farhat (1997, 2000), Farhat and Lee (1998) and Lee and Farhat (2001) we use the dynamics of quadratic logistic maps (Figs. 1 and 2, Eq. (1)) (Holmgren, 1996; Ott, 1993) as an abstract model of a chaotic processing element

$$x_{t+1} = Rx_t(1 - x_t) \tag{1}$$

Bifurcation diagrams of QLM and modified HHM of thermal neurons are shown in Fig. 1(a) and (b). The reasons of their striking resemblance are saddle-node, period-doubling and other common basic bifurcations which underlie these dynamics. Period-doubling cascade route to chaos present in both of them is one of the fundamental bifurcation scenarios which is behind a huge number of processes—from a population dynamics in ecological systems, to chemical reactions, like the one of Belousov-Zhabotinsky (Kaneko & Tsuda, 2000). Computational abilities of the bifurcation processes in the logistic maps' dynamics have been studied extensively in a number of works (Farhat, 1997, 2000; Farhat & Eldefrawy, 1992; Farhat et al., 1994; Lysetskiy et al., 2002). In this article, we focus on one of the numerous bifurcation processes–collapse of chaos to a period-3 orbit in the QLM dynamics and its potential computational properties.

1.2. Dynamics

Here, we briefly review the QLM dynamics which is used in the following sections. With bifurcation parameter $R < 3$, the system $x_{t+1} = f[x_t]$ (Eq. (1)) has a single stable fixed point (Fig. 1(b)). First period-doubling bifurcation occurs when $R = 3$. With R increasing further, the system undergoes period-doubling cascade and at the critical point

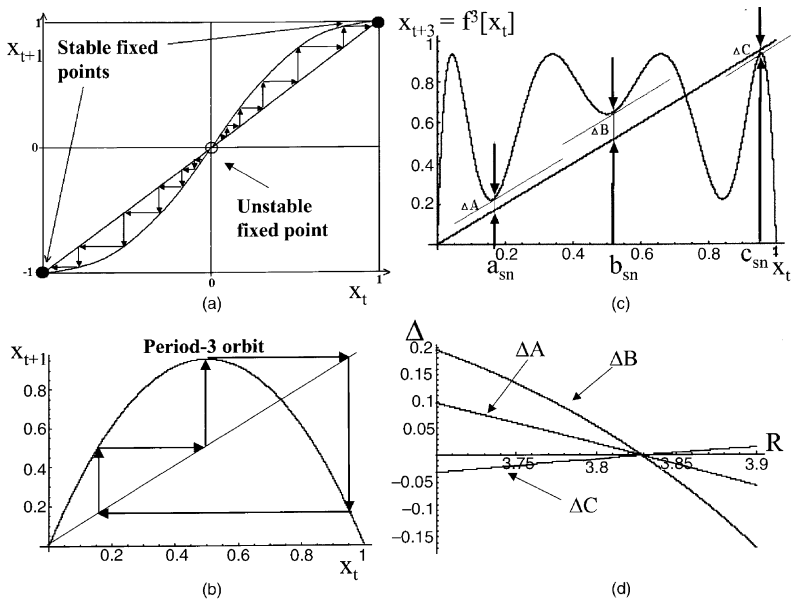

Fig. 2. (a) A neuron with a sigmoidal activation function as a logistic map and its dynamics. (b) Example of quadratic logistic map $x_{t+1} = Rx_t(1 - x_t)$ dynamics: period-3 orbit. (c) Third iterate of QLM $x_{t+3} = f^3[x_t] = f[f[f[x_t]]]$, $R = 3.75$: three stable fixed points are about to be born via bifurcations. (d) The distances ΔA, ΔB, and ΔC (Eq. (5)) to the corresponding bifurcation points a_{sn}, b_{cn} and c_{sn} (Eq. (3)) are identical only for a single critical value of R (in this working range of R).

$R_c \approx 3.57$ it becomes chaotic. Due to the fractal structure of the bifurcation diagram, there is an infinite number of values of R, at which chaotic attractors the system lives on collapse, producing stable periodic orbits.

In this article, we focus on the period-3 orbit which emerges when $R_3 \approx 3.828$ (Fig. 1(b) and (c)). Its appearance is due to three saddle-node bifurcations, giving birth to three stable and three unstable orbits out of chaos. How this phenomena happen can be easily seen graphically. Period-3 orbit of the map $f[x_t]$ (Fig. 2(b)) corresponds to a period-1 orbit (fixed point) of the map $f^3[x_t] = f[f[f[x_t]]]$ (Fig. 2(c)). Fixed point x^* of the system $x_{t+3} = f^3[x_t]$ can be defined as a point of intersection of curves $x_{t+3} = f^3[x_t]$ and $x_{t+3} = x_t$ (Figs. 2(c) and 3). Stability of x^* is defined by Eq. (2a–c)

$$\left|\frac{\mathrm{d}f^3[x]}{\mathrm{d}x}\right| < 1; \tag{2a}$$

$$\left|\frac{\mathrm{d}f^3[x]}{\mathrm{d}x}\right| = 1; \tag{2b}$$

$$\left|\frac{\mathrm{d}f^3[x]}{\mathrm{d}x}\right| > 1; \tag{2c}$$

Fixed point x^* is stable, neutral or unstable if, respectively, condition (2a), (2b) or (2c) is satisfied.

When R is slightly less than R_3, map $f^3[x]$ has no stable fixed points and its state wanders within chaotic attractor (Figs. 1(c) and 2(c)). However, if $R = R_3$, the curve $x_{t+3} = f^3[x_t]$ touches the line $x_{t+3} = x_t$ simultaneously in three saddle-node bifurcation points a_{sn}, b_{cn} and c_{sn}, defined by Eq. (3)

$$\frac{\mathrm{d}f^3[x]}{\mathrm{d}x} = 1 \tag{3}$$

This produces three neutral fixed points via three saddle-node bifurcations. The points, then, split into to three stable and three unstable solutions. We name them correspondingly A_s, B_s, C_s and A_u, B_u, C_u. The stable solutions exist while they satisfy Eq. (2a), but as R further increases they loose their stability via period-doubling bifurcations.

2. Input-induced bifurcations

2.1. Dynamics

In order to make the emergence of stable orbits compute, we shift function $f^3[x]$ vertically with input I (with weight w)

$$x_{t+3} = f^3[x_t] - wI \tag{4}$$

With this input, which is an additional bifurcation parameter, the system demonstrates quite different dynamics and bifurcation scenario. With $R < R_3$ it has no stable fixed points and lives on a chaotic attractor. Now, if we increase I starting from $I = 0$, the curve $x_{t+3} = f^3[x_t] - wI$ will touch the $x_{t+3} = x_t$ line at three distinct input values (Fig. 3). This happens because with

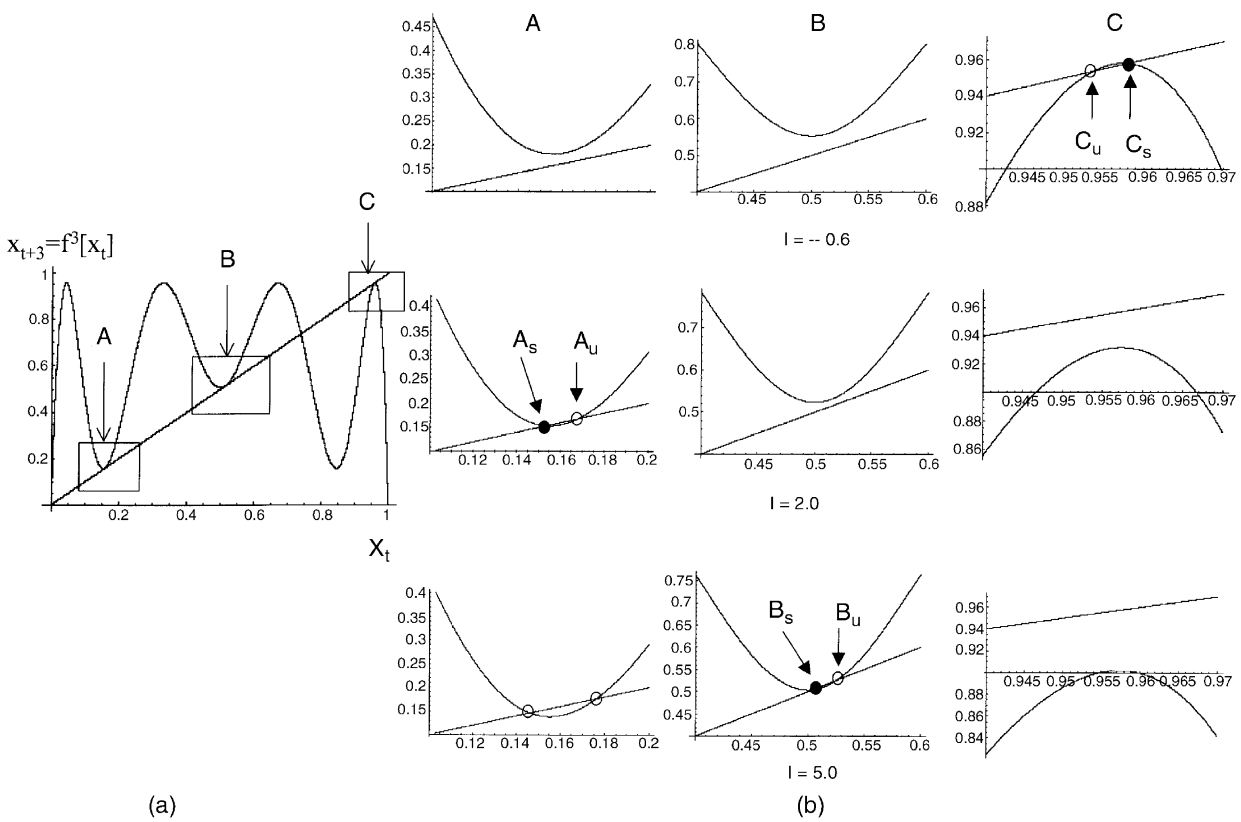

Fig. 3. (a) Function $x_{t+3} = f^3[x_t] = f[f[f[x_t]]] - wI$ of QLM3, $R = 3.805$. (b) Emergence and disappearance of fixed points via sequence of saddle-node bifurcations with different inputs. Black and empty circles correspond, respectively, to stable and unstable fixed points.

the same R the distances

$$\Delta A = f^3[a_{sn}] - a_{sn} \qquad \Delta B = f^3[b_{sn}] - b_{sn}$$
$$\Delta C = f^3[c_{sn}] - c_{sn} \tag{5}$$

at the bifurcation points a_{sn}, b_{sn} and c_{sn} (defined by Eq. (3)) are different (see Fig. 2(c) and (d)). The distances ΔA, ΔB, and ΔC are defined as the solutions of the equation

$$\Delta = f^3[x^*, R^*] - x^* \tag{6}$$

with a given R^* and x^*. Generally, Eq. (6) has multiple solutions. However, in the range of R we are interested in, the solution of Eq. (6) with x^* equal to a_{sn}, b_{sn} and c_{sn} and given R^* are unique, except for $R = R_3$, when $\Delta A = \Delta B = \Delta C = 0$ (Fig. 2(d)).

Thus, the shift $wI = \Delta A$ induces a single saddle-node bifurcation: the curve $x_{t+3} = f^3[x_t] - wI$ touches the line $x_{t+3} = x_t$ at a single point $x_t = a_{sn}$. It splits then into stable fixed point A_s and unstable A_u (Fig. 3b: column A, $I = 2.0$) when the shift is increased. The chaotic attractor collapses and the state of the system converges to A_s, as is shown in Fig. 4 ($I = 1.81$).

As I keeps increasing, A_s looses its stability via period-doubling bifurcation according to Eq. (2c). Dynamics of x undergoes cascade of these bifurcations and becomes chaotic (Fig. 4). Then, when the shift $wI = \Delta B$, another stable point B_s emerges via saddle-node bifurcation (Fig. 3b: Column B, $I = 5.0$). At this moment (chaotic) dynamics of x converges to the stable point B_s. (Figs. 3(b) and 4). The same bifurcation mechanism underlies the emergence of the stable fixed point C_s (and then, the loss of its stability) when I is negative, and the function $f^3[x]$ is shifted upward.

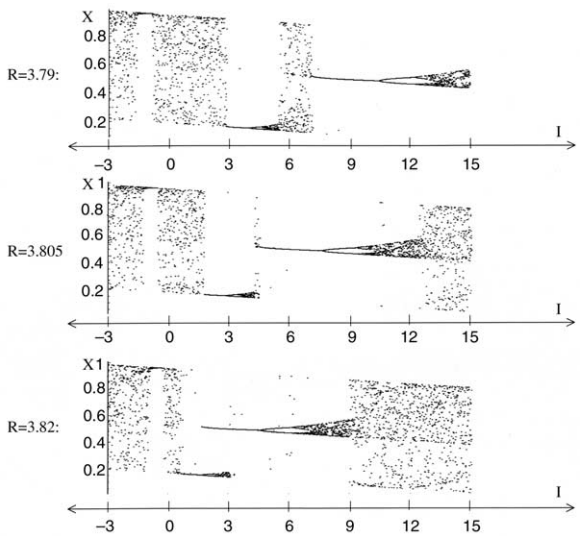

Fig. 4. Dynamics of the map $x_{t+3} = f^3[x_t] - wI$ with $R = 3.805$, versus I. Three input intervals are mapped onto three stable fixed points A, B and C.

Let I_{sn} and I_{pd} be the inputs that produce, correspondingly, a stable fixed point via saddle-node bifurcation (Eq. (2a)) and loss of its stability via period-doubling bifurcation (Eq. (2c)). The map's dynamics at the critical points A, B and C can be seen, then, as an analog of a perceptron, as it divides the input interval into two subintervals. One of them produces a stable fixed point and is defined as

$$I_{sn} < |I| < I_{pd} \tag{7}$$

where sign of I is the same as of the corresponding distance Δ (6). The inputs outside of this interval do not invoke a fixed point and the system remains chaotic or stays on a periodic orbit.

It should be noted that extension of the system for the case when **I** and **w** are vectors is rather straightforward. The QLM3 neuron $x_{t+3} = f^3[x_t] - \sum w_j I_j$ maps multidimensional space to the induced stable fixed point in the same way as it does with one-dimensional input (Fig. 4).

2.2. Simulation

In the following simulation example bifurcation parameter is set at $R = 3.808$. The reason behind this choice is that the widest period-3 orbit in the map's dynamics (Fig. 1(b) and (c)) emerges with $R_3 = 3.828$; $R_0 = 3.808$ is slightly less than R_3, so the system is chaotic, but its stable states can be produced by a small input.

The saddle-node bifurcation points, at which the curve $x_{t+3} = f^3[x_t] - wI$ touches $x_{t+3} = x_t$ line are defined by Eq. (2b): $a_{sn} = 0.1604$, $a_{pd} = 0.1501$, $b_{sn} = 0.5157$, $b_{pd} = 0.4851$, $c_{sn} = 0.9556$, $c_{pd} = 0.9588$. Input intervals Eq. (7) that produce emergence of fixed points A, B and C (with $w = 0.01$) are calculated with Eq. (2b and c) as follows

$$\begin{aligned} A &: I^A_{sn} = 1.81 < I < I^A_{pd} = 3.02 \\ B &: I^B_{sn} = 4.51 < I < I^B_{pd} = 7.48 \\ C &: I^C_{sn} = -0.53 > I > I^C_{pd} = -0.91 \end{aligned} \tag{8}$$

Simulation results (Fig. 4) demonstrate that QLM3 neuron maps the set of input intervals onto the set of invoked stable fixed points A, B and C.

It should be noted that if $I \neq 0$ the map $x_{t+3} = f^3[x_t] - wI$ no longer maps the interval [0,1] on itself. Two 'runaway' regions appear at the edges of the interval [0,1]. They are defined as: $0 < x < x_c$ and $1 - x_c < x < 1$, where x_c is the leftmost solution (for $x_c \in [0, 1]$) of equation $f^3[x^*] - wI = x^*$ if the shift is downward ($I > 0$), and x_c is its rightmost solution (for $x_c \notin [0, 1]$) if $I < 0$. In our simulations, where the input maximum, $I_{max} = 15$ is positive and $R = 3.805$, the critical value $x_c = 2.9 \times 10^{-3}$, which slightly restricts the set of initial conditions to $[x_c, 1 - x_c]$.

3. Learning

The sizes and centers of the intervals mapped by QLM3 neuron to its output states depend on R (Eqs. (6) and (8), Fig. 5) and w. To adjust w, one of the learning algorithms for the multilevel neurons would be appropriate, for example, the one described in Malinowski, Cholewo, and Zurada (1995).

We focus on the other option provided by QLM3 neuron—the learning of the bifurcating parameter R. It

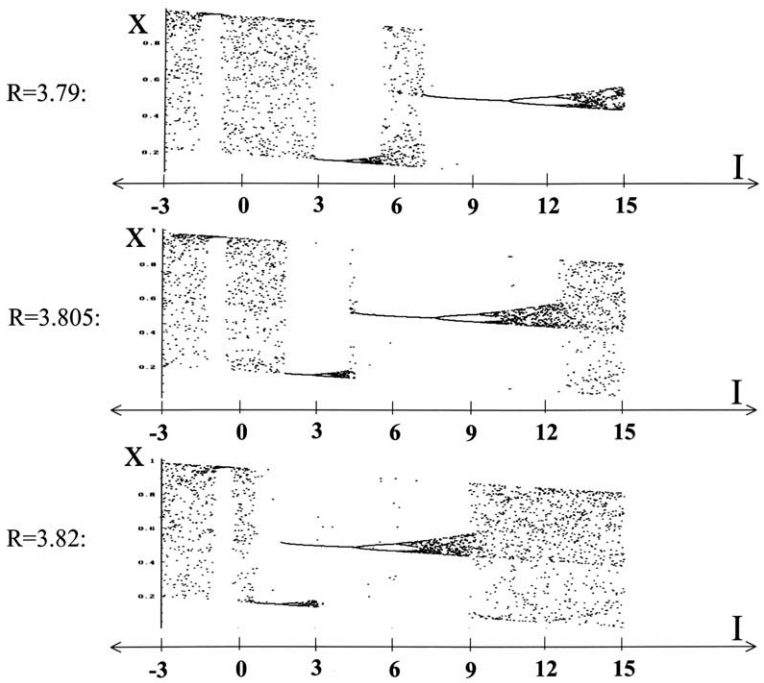

Fig. 5. Parameter-depending mapping: examples of the input intervals inducing stable fixed points with different values of bifurcation parameter R.

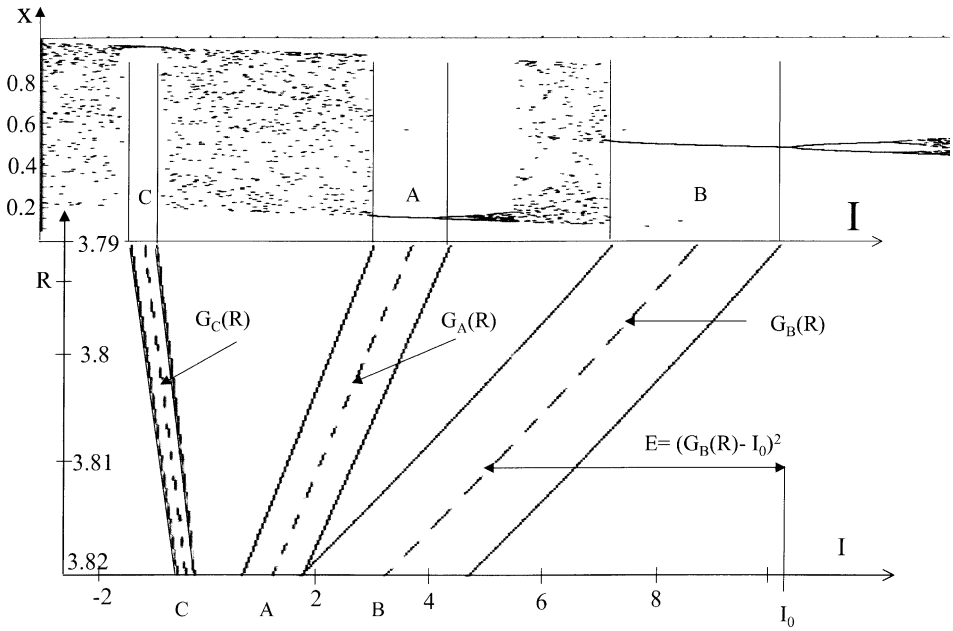

Fig. 6. The mapping of the input interval as a function of bifurcation parameter R.

is, in a sense, analogous to the optimizing the steepness of the activation function of a sigmoidal neuron to maximize the information of its output (Bell & Sejnowski, 1995).

The mapping of QLM3 neuron as a function of R is shown in Fig. 6, where the centers of mapped intervals (also functions of R) are described as curves $G_A(R)$, $G_B(R)$, $G_C(R)$. To make an input I_0 produce a desired output, for example a stable state A, R should be adjusted in a way to put I_0 into the interval mapped to A : $I^A_{\text{sn}}(R) < I_0 < I^A_{\text{pd}}(R)$ (Eq. (7)). Defining it more strictly, we want the input to be in the center of this interval, $I_0 = G_A(R)$, defined with Eqs. (5) and (9) as

$$G_A(R) = \frac{1}{2}(I^A_{\text{sn}}(R) + I^A_{\text{pd}}(R)) = \frac{1}{2}((f^3[a_{\text{sn}}, R] - a_{\text{sn}}) + (f^3[a_{\text{pd}}, R] - a_{\text{pd}})) \quad (9)$$

Thus, learning of mapping I_0 to A transforms to the task of minimizing the distance $|I_0 - G_A(R)|$ (Fig. 6). The error function can, then, be defined as a square of this distance

$$E(R) = (I_0 - G(R))^2 \quad (10)$$

This brings the error gradient learning rule to the following form

$$\Delta R = -c\frac{\mathrm{d}E}{\mathrm{d}R} = 2c(I_0 - G(R))G'(R) \quad (11)$$

where $G'(R)$ stands for the derivative of $G(R)$ and c is the learning coefficient.

To implement unsupervised learning the learning algorithm has to choose the centerline $G_J(R)$ which is closest to the applied input I_0: $E_J = \min_j [E_j], j\{ \in A, B, C\}$, and then the error E_J has to be minimized. In the case of supervised learning the corresponding centerline is defined by the teacher's signal.

Examples of simulations of the proposed learning algorithm (Eq. (11)) are shown in Fig. 7. The task was to learn mapping of input $I_0 = 6$ to the desired output B. With initial conditions $R_0 = 3.77$ and $R_0 = 3.82$ this input produces chaotic and period-2 orbits, respectively (Fig. 6). After 70 learning steps (Eq. (11)) R converged to $R = 3.805$ (Fig. 7(a)) and it produced desired output B (Figs. 4 and 5) with the errors $E = 6.7 \times 10^{-4}$ and $E = 4.4 \times 10^{-4}$ respectively. Dynamics of E is shown in Fig. 7(b). The learning coefficient used $c = 2 \times 10^{-6}$.

Thus, this learning method enables the QLM3 neuron to adjust adaptively its bifurcation parameter R to map certain input intervals to specific stable states (classes). The upgrade of R changes the mapping of all intervals/clusters (three, in our case) simultaneously (Figs. 5 and 6).

4. Discussion

This article explores computational abilities of controlling the collapse of a chaotic attractor to the stable orbits in the dynamics of a quadratic logistic map. Such control is implemented with an external input (additional bifurcation parameter) to the third iterate of QLM. The resulting processing unit, QLM3 neuron, demonstrates a richer repertoire of behavior than a classical artificial neuron with sigmoidal activation function. Besides saturated regions, where inputs from certain intervals/clusters invoke different stable states, QLM3 neuron also produces chaotic

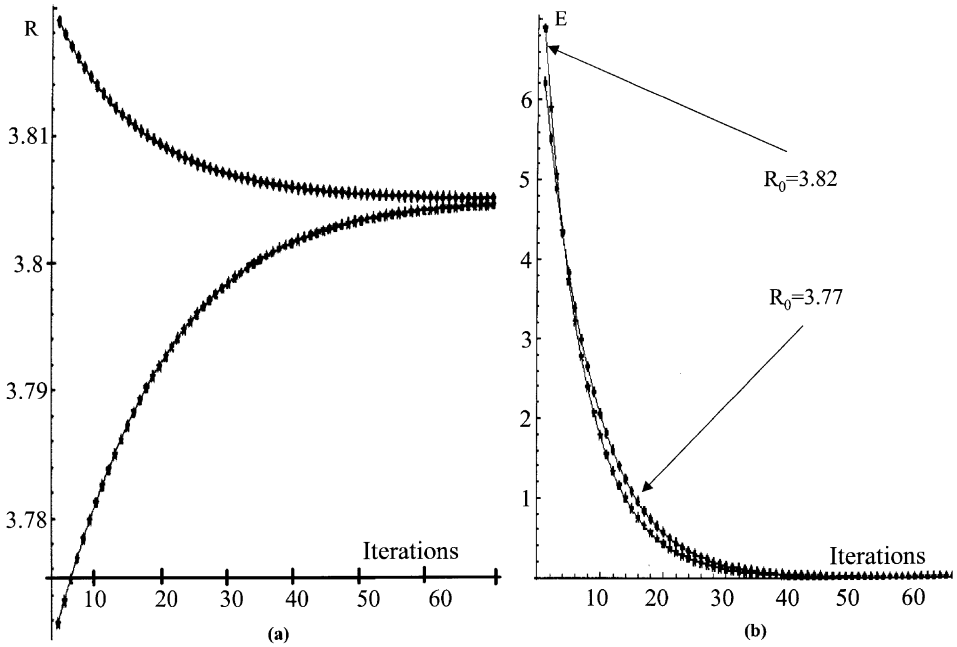

Fig. 7. (a) Dynamics of the bifurcation parameter R during learning. (b) Error E during learning.

or periodic dynamics in response to the rest of the inputs. Another potentially useful property of the QLM3 neuron is its ability to adjust adaptively its mapping by learning the bifurcation parameter value.

In this article, we used the emergence of period-3 orbit out of chaos which happens at $R \approx 3.828$. However, the appearances of a period-n orbit out of chaos, or, in other words, transitions of nth iterate from chaos to n fixed points are ubiquitous in the quadratic map's dynamics. For example, in the range of R from $R_c \approx 3.57$ (when the map's dynamics first becomes chaotic) to $R = 4$, there exist $(2^p - 2)/2p$ windows of period p orbits, where p is a prime number (Ott, 1993).

The map of nth iterate would look structurally similar to the map of the third iterate shown in Fig. 2(c), but it would have n saddle-node bifurcation points instead of 3. So, it would be possible to construct a QLM based neuron with a large number of stored stable states using other periodic orbits. It might be easier, though, to artificially generate a map with required number of saddle-node bifurcations.

Acknowledgements

This work was sponsored by the Department of the Navy, Office of Naval Research, Grant N000 14-01-1-0630. The content of this information does not necessarily reflect the position of the government.

We would like to thank Andrzej G. Lozowski for critical discussions and valuable comments on this manuscript. We also express thanks to the anonymous reviewers and the action editor, who have provided many insightful comments helpful for revision of this paper.

References

Adachi, M., & Aihara, K. (1997). Associative dynamics in a chaotic neural network. *Neural Networks*, *10*(1), 83–98.

Bell, A. J., & Sejnowski, T. (1995). An information–maximization approach to blind separation and blind deconvolution. *Neural Computation*, *7*, 1129–1159.

Braun, W., Eckhardt, B., Braun, H. A., & Huber, M. (2000). Phase–space structure of a thermoreceptor. *Physical Review E*, *62*(5), 6352–6360.

Dmitriev, A., Shirokov, M., & Starkov, S. (1997). Chaotic synchronization in ensembles of coupled maps. *IEEE Transactions on Circuits and Systems I: Fundamental Theory and Applications*, *44*(10), 918–926.

Ermentrout, G. B., & Kopell, N. (1998). Fine structure of neural spiking and synchronization in the presence of conduction delays. *Proceedings of the National Academy of Sciences*, *95*(3), 1259–1264.

Farhat, N. (1997). Dynamical networks with bifurcation processing element (pp. 265–268). *Proceedings of the International Symposium on Nonlinear Theory and its Applications (NOLTA'97), Honolulu, HI.*

Farhat, N. (2000). Cortitronics: the way to designing machines with brain-like intelligence (*Vol. 4109*) (pp. 103–109). *Proceedings of SPIE*, Bellingham, WA: SPIE.

Farhat, N., & Eldefrawy, M. (1992). The bifurcating neuron: characterization and dynamics (*Vol. 1773*) (pp. 23–35). *In Photonics for computers, neural networks, and memories*, Bellingham, WA: SPIE.

Farhat, N., Lee, G. H., & Ling, X. (1998). Dynamical networks for ATR (pp. D1–D4). *Proceedings of RTO SCI Symposium on Non-Cooperative Air Target Identification Using Radar, published in RTO MP6, Mannheim, Germany*.

Farhat, N., Lin, S.-Y., & Eldefrawy, M. (1994). Complexity and chaotic dynamics in a spiking neuron embodiment (*Vol. CR55*) (pp. 77–88). *In Adaptive computing: Mathematics, electronics, and optics*, Bellingham, WA: SPIE.

Feudel, U., Neiman, A., Pei, X., Wojtenek, W., Braun, H., Huber, M., & Moss, F. (2000). Homoclinic bifurcation in a Hodgkin-Huxley model of thermally sensitive neurons. *Chaos*, *10*(1), 231–239.

Freeman, W. (1988). Strange attractors that govern mammalian brain dynamics shown by trajectories of electroencephalographic (EEG) potential. *IEEE Transaction on Circuits and Systems*, *35*, 781–783.

Fukai, H., Doi, S., Nomura, T., & Sato, S. (2000). Hopf bifurcations in multiple-parameter space of the Hodgkin-Huxley equations I. Global organization of bistable periodic solutions. *Biological Cybernetics*, *82*, 215–222.

Gilmore, R., Pei, X., & Moss, F. (1999). Topological analysis of chaos in neural spike train burst. *Chaos*, *9*(3), 812–817.

Hirsch, M., & Baird, B. (1995). Computing with dynamic attractors in neural networks. *Biosystems*, *34*, 173–195.

Holden, A. V., Hyde, J., Muhamad, M. A., & Zhang, H. G. (1992). In J. G. Taylor, & C. L. T. Mannion (Eds.), *Bifurcating neurons* (pp. 41–80). *Coupled oscillating neurons*, London: Springer.

Holmgren, R. A. (1996). *A first course in discrete dynamical systems*. New York: Springer.

Hoshino, O., Usuba, N., Kashimori, Y., & Kambara, T. (1997). Role of itinerancy among attractors as dynamical map in distributed coding scheme. *Neural Networks*, *10*(8), 1375–1390.

Izhikevich, E. M. (2000). Neural excitability, spiking and bursting. *International Journal of Bifurcation and Chaos*, *10*, 1171–1266.

Kaneko, K., & Tsuda, I. (2000). *Complex systems: Chaos and beyond*. New York: Springer.

Koch, C. (1999). *Biophysics of computation: Information processing in single neurons*. New York: Oxford University Press.

Lee, G., & Farhat, N. H. (2001). The bifurcating neuron network 1. *Neural Networks*, *14*, 115–131.

Lysetskiy, M., Lozowski, A. G., & Zurada, J. M. (2002). Bifurcation-based neural computation (pp. 2716–2720). *Proceedings of the IEEE International Joint Conference on Neural Networks, Honolulu, HI, May 12–17*.

Malinowski, A., Cholewo, T. J., & Zurada, J. M. (1995). Capabilities and limitations of feedforward neural networks with multilevel neurons (*Vol. 1*) (pp. 131–134). *Proceedings of the IEEE International Symposium on Circuits and Systems, Seattle, WA, April 30–May3*.

Ott, G. (1993). *Chaos in dynamical systems*. New York: Cambridge University Press.

Rabinovich, M., Volkovskii, A., Lecanda, P., Huerta, R., Abrabanel, H. D. I., & Laurent, G. (2001). Dynamical encoding by network of competing neuron groups: winnerless competition. *Physical Review Letters*, *87*, 068102.

Sinha, S., & Ditto, W. L. (1998). Dynamics based computation. *Physical Review Letters*, *81*(10), 2156–2159.

Tokuda, I., Nagashima, T., & Aihara, K. (1997). Global bifurcation structure of chaotic neural networks and its application to traveling salesman problems. *Neural Networks*, *10*(9), 1673–1690.